5/20/2014

Further Advances in Simulating the Processing of Composite Materials by Electromagnetic Induction

M. Duhovic, M. Hümbert, P. Mitschang, M. Maier
Institut für Verbundwerkstoffe GmbH, Erwin-Schrödinger-Str., Building 58
67663 Kaiserslautern, Germany
P. L'Eplattenier , I. Çaldichoury
Livermore Software Technology Corporation, 7374 Las Positas Road, Livermore,
CA 94551, USA

Abstract

Continuous induction welding is an advanced material processing method with a very high potential of providing a flexible, fast and energy efficient means of joining together thermoplastic composites to themselves and metal alloys. However, optimization of the process is very difficult as it involves the interaction of up to four different types of physics. In the previous installments of this work, static plate heating and continuous induction welding simulations of carbon fiber reinforce thermoplastic (CFRTP) plates were presented looking in particular at point temperature measurements and 3D surface plots of the in-plane temperature distribution across the entire width of the joint on the top as well as the joining interface of the laminate stack. In this paper, static plate heating tests are once again revisited and the importance of through the thickness temperature behavior is considered. For a single plate, the through thickness temperature profile follows a predictable pattern when using an induction frequency producing a skin depth of the same thickness as the plate. For two stacked but unconnected plates, the temperature profile becomes less obvious, in particular for plate stacks of different thicknesses. By correctly simulating the through thickness temperature profile the heating behavior can be ultimately controlled via top surface air-jet cooling together with other induction equipment parameters giving an optimum heating effect at the joining interface. In addition, further developments in the induction heating electromagnetism module available in LS-DYNA® R7 are examined including the inclusion of an orthotropic electromagnetic material model as well as electrical contact and its resulting contact resistance and effect on the overall heating behavior.

1-Introduction

As the aerospace industry pushes the use of composite materials in commercial aircraft to beyond 50% of the total structural weight (Boeing 787 and Airbus A350), the automotive industry can catch a glimpse as to what is in store for them in the near future. Carbon fiber reinforced thermoplastic plastics (CFRTPs) combined with advanced metal alloys represent the next logical step in material selection in order to meet future energy efficiency goals and lightweight design criteria.

An important part of the vehicle body construction is joining. Joining methods for metallic passenger cells and chassis components include automated robotic spot and seam welding of pre-stamped parts along with glueing in some areas mainly for providing water sealing properties.

For the use of fiber reinforced thermoplastic parts to be accepted in the automotive industry, the ability for the material to be joined quickly and efficiently by robotic means in a controlled manner giving excellent bond strength between the connected parts needs to exist. All the aforementioned features can be provided by induction welding technology.

2-Short overview of induction welding

Induction welding is a materials joining process that uses an oscillating electromagnetic field to generate a contact-free heating. The subsequent fusion bonding which occurs in the case of thermoplastic composite joints is supported by applying pressure and allowing enough time for intermolecular diffusion to take place. Thermoplastic composite to metal joints are also possible utilizing similar processing conditions, although the bond in this case is created through different adhesion mechanisms. During the process, an induction coil, connected to a high frequency oscillating current source (usually in the kHz – MHz range) creates an alternating current in the coil. This current in turn produces a time-variable magnetic field of the same frequency in the near surroundings of the coil as illustrated in Figure 1.

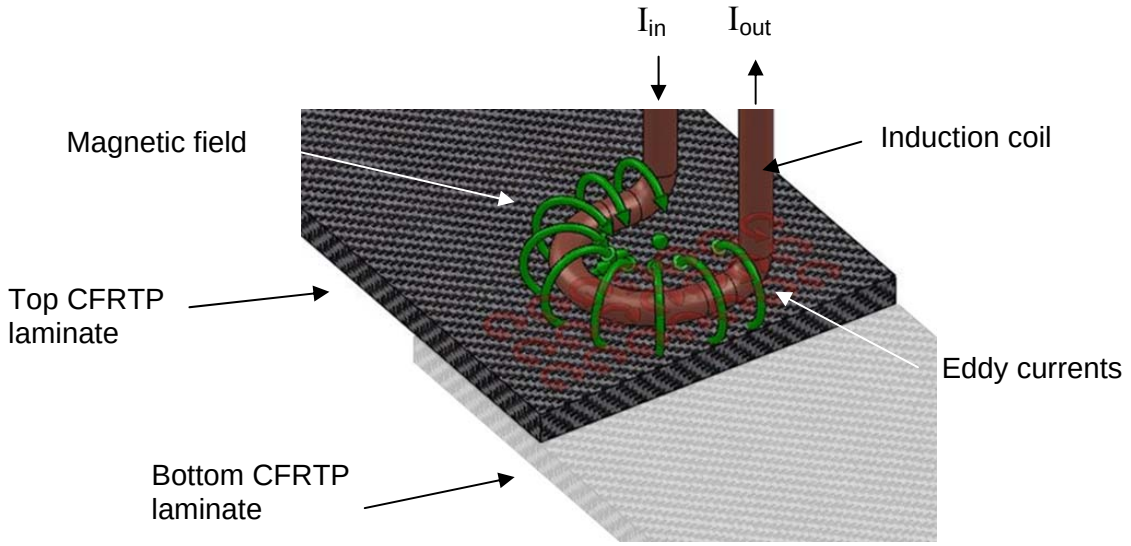

Figure 1: *Working principle of induction heating in weave structured CFRTP sheet materials (image courtesy of Mrs. Mirja Didi IVW GmbH)*

The alternating magnetic field induces oscillating eddy currents in a work piece when placed in close proximity to the coil. Heat energy is generated via the Joule effect as a result of the induced eddy currents flowing through the electrically conductive material [1, 2]. For composite materials containing glass fiber reinforcements, no Joule heating can occur and a susceptor material in the form of a steel mesh or electrically conductive polymer film, for example, is required between the materials to be joined. Composites containing carbon fibers in certain configurations (weaves) however, produce a significant Joule heating effect and can be utilized to achieve the necessary heating effect. During a finite element simulation of the induction welding process of thermoplastic composites, it is precisely the Joule heating phenomena which is of primary interest and is simulated.

3-Static plate through thickness heating experiments

In order to investigate the through thickness temperature distributions during induction heating and more importantly induction welding, static plate heating experiments have been performed. Although the findings cannot be directly transferred to the continuous heating (moving coil) case, they can provide a useful insight into joule heating phenomena for different plate thicknesses and the possible effects of a contact resistance between the plates. For all the experiments, carbon fiber reinforced polyphenylene sulfide (CF-PPS) was used. The experimental setup for static plate heating measurements is shown in Figure 2.

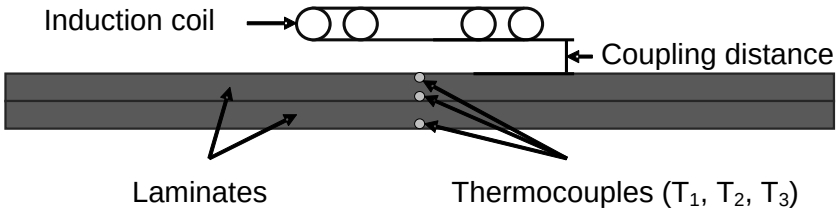

Figure 2: *Schematic of double laminate static heating test performed using 2x1 and 2x2 mm thick CF-PPS plates*

A pancake type coil identical to that used in previous works [3, 4] was again used to heat either a fully connected (consolidated) or unconnected stack of two CF-PPS laminates. In order to measure the temperature, three thermocouples were used, one on top of the upper laminate (temperature T_1), one between the two laminates (temperature T_2) and one on the bottom of the lower laminate (temperature T_3). The experiments were carried out for laminates with a thickness of 1 mm and 2 mm. Moreover three different generator powers (10%, 20%, 30%) and two different coupling distances (5 and 10 mm) were used. The results for an unconnected stack of two laminates with a thickness of 1 mm at a coupling distance of 10 mm are shown in Figure 3.

The specimens were always heated until the top laminate reached 250°C. The experiments confirmed the previously assumed temperature distribution. The top laminate is heated the most and the temperature drops with increasing distance to the coil. A similar behavior was observed when the coupling distance was reduced to 5 mm as shown by the results in Figure 4.

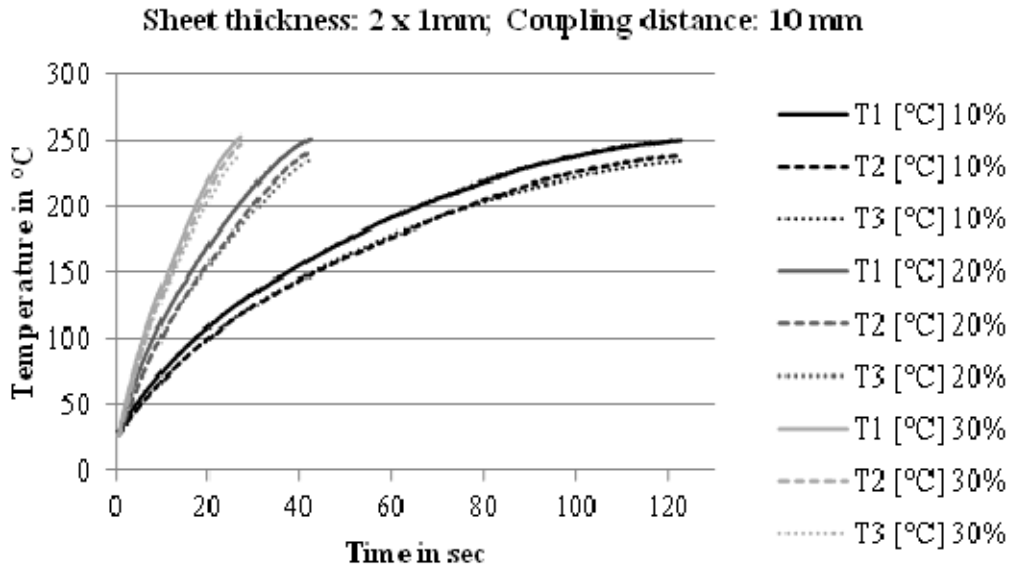

Figure 3: *Static heating results for two laminates with a thickness of 1 mm and a coupling distance of 10 mm*

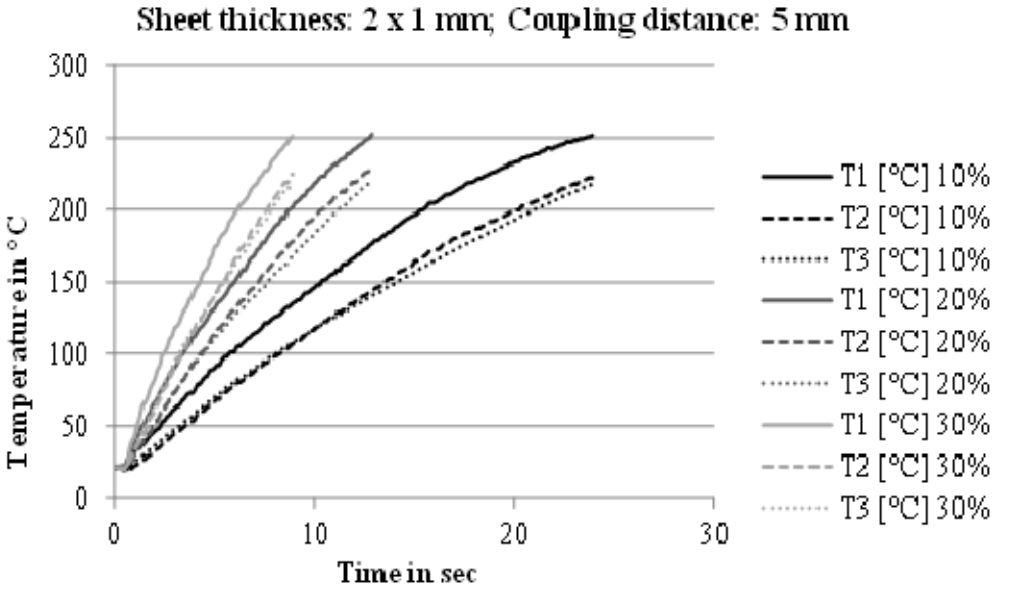

Figure 4: *Static heating results for two laminates with a thickness of 1 mm and a coupling distance of 5 mm*

A comparison of the heating times shows that a reduction of the coupling distance by 50% can lead to a reduction in heating time of up to approximately 75%. At a power of 10% the heating times was reduced from 120 s to 30 s. The reason for this lies in the fact that the magnetic field intensity drops with increasing distance to the coil as predicted by the Biot-Savart law. Moreover it can be observed, that the difference in temperature between the top of the upper laminate and the two other measuring points decreases when either the coupling distance is increased or the power is decreased.

The results of Figures 3 and 4 can be compared to the case where two 1 mm plates have been fully consolidated together, in effect representing a single uniform 2 mm thick plate. Figure 5 shows this for a coupling distance of 10 mm. It can be seen compared to Figure 3 that the time required to heat the top laminate to 250°C is now slightly lower at all powers. In addition, a strange effect in the order of the temperatures can be observed where the T_2 thermocouple in the center of the laminate measures a lower temperature that thermocouple T_3 on the bottom surface. This can be explained by the fact that the thermocouples cannot be placed in the exact same position through the thickness and may coincide exactly or be slightly away from a junction (fiber crossover) heating location. It is also believed that regardless of the Biot-Savart law, the low electrical conductivity of the material results a skin depth giving a fairly uniform volumetric heating.

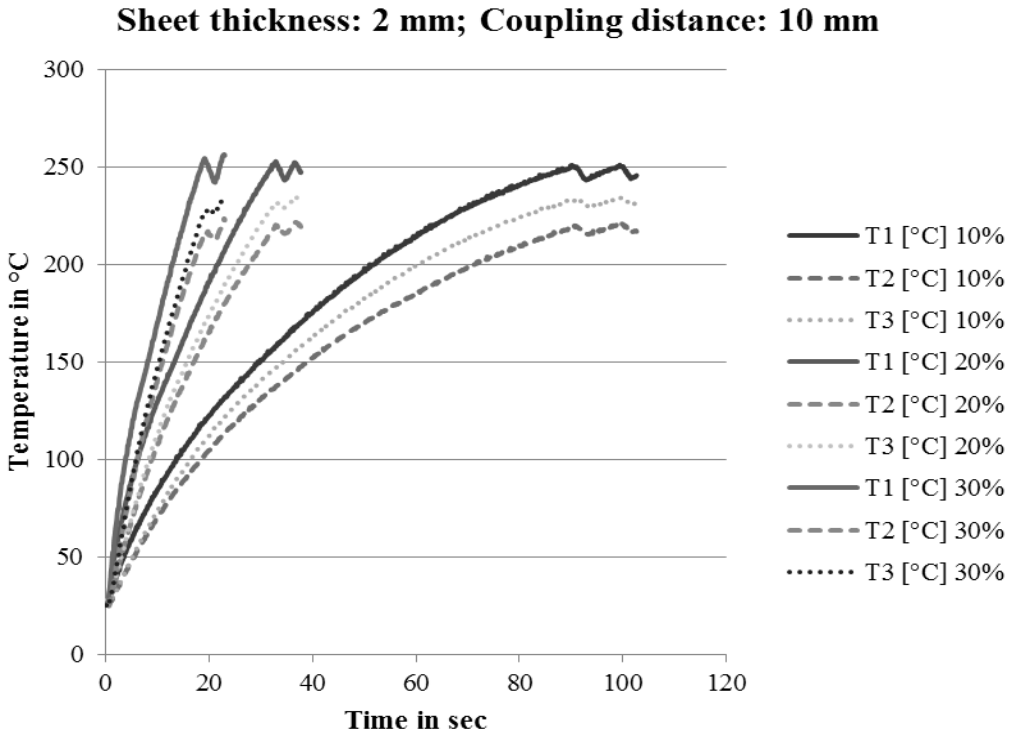

Figure 5: *Static heating results for a single laminate with a thickness of 2 mm and a coupling distance of 10 mm*

In Figure 6, with a coupling distance of 5 mm, the switch in the expected trend between the T_2 and T_3 thermocouples is amplified since the same specimen was used to perform the test. The results highlight the difficulty in measurement due to the discontinuous in-plane temperature pattern that results (particularly at high powers and small coupling distances) from closely spaced junction heating zones defined by the carbon fiber reinforcement yarn size and weaving pattern. Further experiments are required to be able to assess any additional joule heating influence due to a contact resistance perhaps using a very finely woven carbon fiber reinforcement mesh. From the current results, it can be seen that the overall impact on the Joule heating effect due to an additional contact resistance between the plates should not be very high.

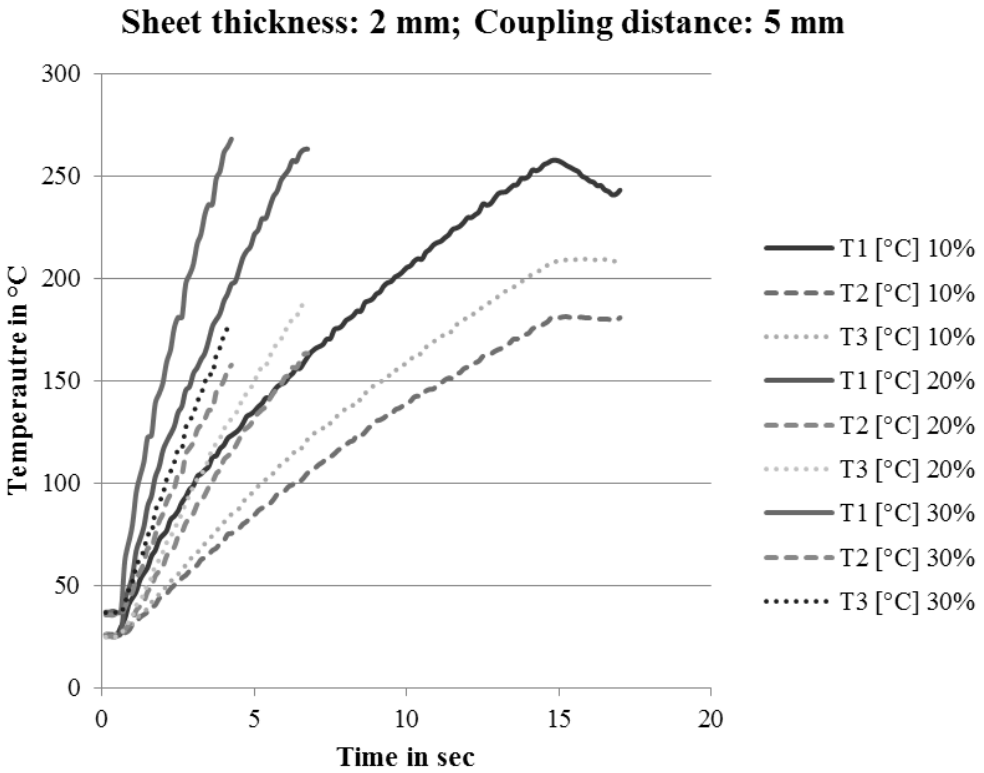

Figure 6: *Static heating results for a single laminate with a thickness of 2 mm and a coupling distance of 5 mm*

The resulting heating curves from the induction heating of two unconnected laminates with a thickness of 2 mm at a coupling distance of 5 mm are shown in Figure 7.

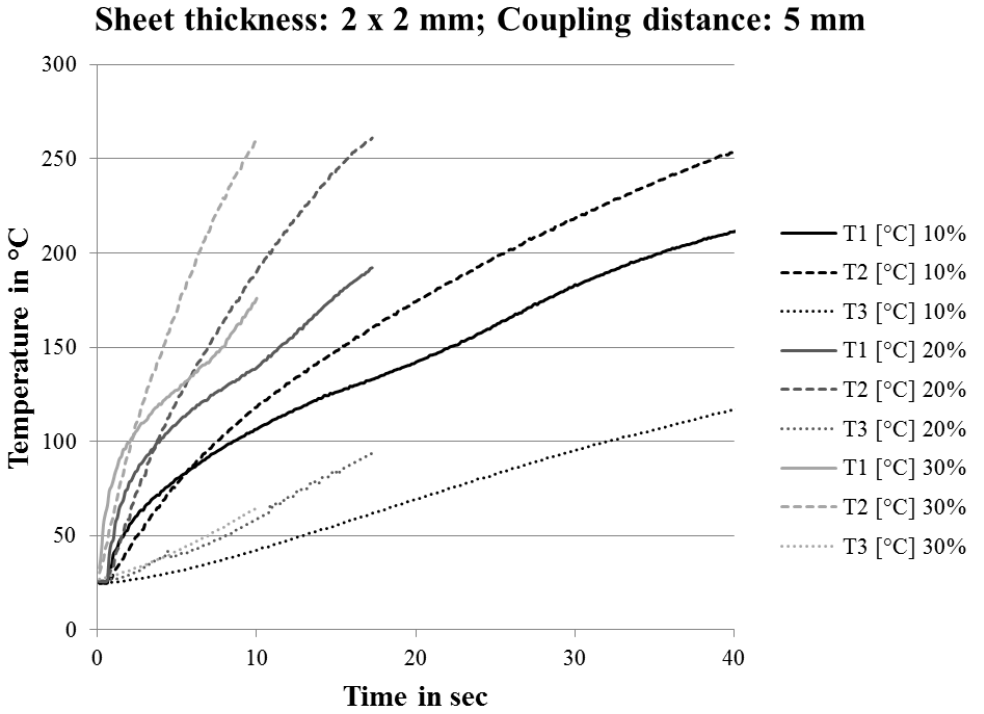

Figure 7: *Static heating results for two laminates with a thickness of 2 mm and a coupling distance of 5 mm*

In this case, it was observed that the temperature T_1 on the top laminate appears to be overtaken by the temperature T_2 between the laminates. It can also be seen that T_3 is now much lower and that a volumetric type heating that was somewhat the case in the 2 x 1 mm tests now no longer occurs. The same trend but with a lower spread between the T_1 _ T_3 temperature curves occurs for a coupling distance of 10 mm albeit over a longer heating time.

Using a new specimen now consolidated into a single 4 mm thick plate, the heating experiments were once again performed for the different coupling distances of 5 and 10 mm as are shown in Figures 8 and 9 respectively.

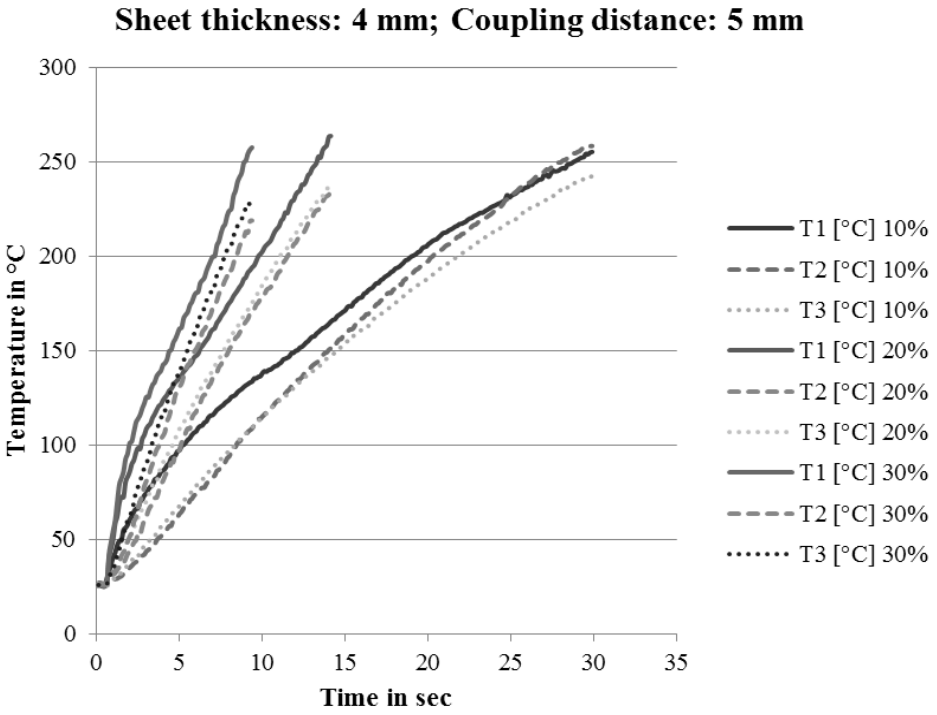

Figure 8: *Static heating results for a single laminate with a thickness of 4 mm and a coupling distance of 5 mm*

Just as was observed for the 2 x 1 mm case, the overall heating time to 250°C in the unconnected 2 x 2 mm specimen compared to a single 4 mm specimen appears to be longer by 20-30%. This seems to be a consistent observation overall in all the experiments and may suggest a kind of electromagnetic shielding effect coupled with a poor thermal conductivity barrier at the interface of the two unconnected laminates. The latter seems unlikely as the thermal conductivity through the thickness of the laminate is already very poor (values used in this work of 0.32 W/m.K as calculated by Moser [5] and which have been measured for such materials by Schuster [6]). While shielding type explanations seem plausible, the reason as to why for the thicker laminate cases, the top laminate temperature T_1 is overtaken by T_2 and even T_3 in the case of 10 mm coupling distance is baffling. Material related effects can be counted out as the same phenomenon has been observed in many different specimens. Equipment and thermocouple effects could be responsible, although regarding the equipment, some changes in the machine parameters during the test cannot account for the switch in temperature order observed.

Thermocouple errors are another possibility due to the influence of the magnetic field, however this has also been studied quite closely and the effects are predictable and can be minimized for certain thermocouple types. Some help through the use of finite element electromagnetic simulations using LS-DYNA R7 as performed in the following section may help shed some light on these issues.

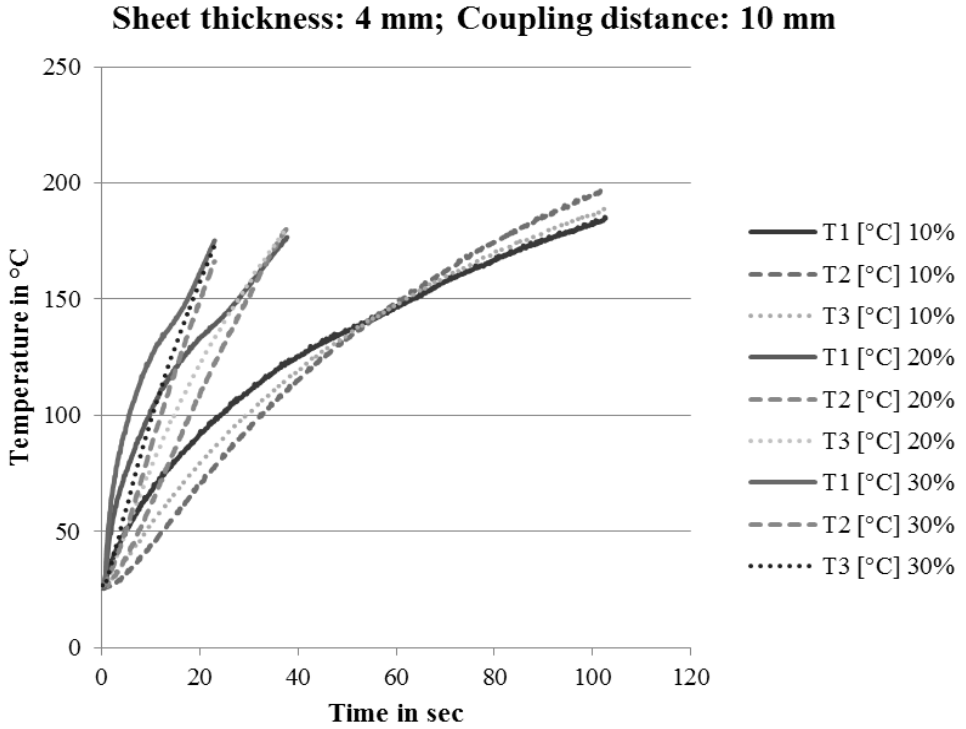

Figure 9: *Static heating results for a single laminate with a thickness of 4 mm and a coupling distance of 10 mm*

4-Modelling induction heating in LS-DYNA R7

4-1 The inductive heating solver in LS-DYNA

The Electromagnetism (EM) solver included in release R7 of LS-DYNA solves the Maxwell equations in the Eddy current (induction-diffusion) approximation [7-9]. This is suitable for cases where the propagation of electromagnetic waves in air (or vacuum) can be considered instantaneous which is the case in most industrial magnetic metal welding, forming or inductive heating applications. The EM solver is strongly coupled with all the other solvers available in LS-DYNA allowing truly multi-physics phenomena to be simulated. EM fields are solved using a Finite Element Method (FEM) for the conductors and a Boundary Element Method (BEM) for the surrounding air/insulators therefore eliminating the need for a surrounding air mesh.

An inductive heating solver was introduced in order to solve the computer cost issue arising when high frequency currents, therefore very small time steps, were combined with long simulation runs (typically, an AC current with a frequency ranging from kHz to MHz and a total

time for the process in the order of a few seconds). The induction heating solver works by assuming a current which oscillates very rapidly compared to the total time of the process. A full eddy-current problem is solved over two full periods with a "micro" EM time step where the EM fields as well as the joule heating is computed.

It is then assumed that the properties of the material (heat capacity, thermal conductivity, magnetic permeability) and mostly the electrical conductivity which drives the flow of the current and the joule heating do not change for the next periods of the current within the "macro" EM time step (or overall solution time step) chosen. The calculated averaged joule heating term is then added many times over to the thermal solver. If the material properties change significantly affecting the EM fields or more accuracy is desired, then more recalculations of the "macro" EM time step can be performed over the entire solution time.

4-2 Material properties

A large number of material properties need to be collected in order to setup the simulations. A summary of the properties used in the LS-DYNA finite element models can be found elsewhere in previous works by Duhovic et al. [10]. Free convection heat transfer coefficients are also taken into account on exposed faces of the plates and are input as tabulated values with respect to temperature (for a range of 40 – 480 °C). Typical average values for free convection are 7.83 W/(m^2.K) for the horizontal upside surface, 5.94 W/(m^2.K) for the horizontal downside surface and 33.00 W/(m^2.K) for the vertical faces.

The "skin effect" is an electromagnetic phenomenon whereby the flow of current concentrates itself on the outer surface of the conducting body. The skin depth is automatically calculated using the formula given in Equation (1), which is a function of the specified electromagnetic material properties. It can be seen that the calculated value may be significant in the present work as the skin depth is quite close to the overall thickness of the laminate stack, i.e. 5.8 mm at 540kHz for CF-PPS.

$$\delta = \sqrt{\frac{2\rho}{(2\pi f)(\mu_o \mu_r)}} \approx 503\sqrt{\frac{\rho}{\mu_r f}} \tag{1}$$

where

δ = the skin depth in meters (calculated using Eq. 1 as 5.8 mm for pancake coil (540 kHz) for CF-PPS)
μ_r = the relative permeability of the medium (1 used for CF-PPS, reference [5])
μ_o = the magnetic permeability of free space ($4\cdot\pi\cdot10^{-7}$ H/m)
ρ = the resistivity of the medium in Ω•m, also equal to the reciprocal of its conductivity:
$\rho = 1 / \sigma$ (for CF-PPS, $\rho = 7.14\times10^{-5}$ Ω•m, reference [5])
f = the frequency of the current in Hz

5-Static plate through thickness induction heating simulations

5-1 Single and double plate induction heating models

Comparisons to the experiments performed in section 3 can be made for both the single and double plate induction heating cases. Figures 10 a) and b) show example models of the single and double (100 x 100 x 2 mm) CF-PPS static plate induction heating simulations respectively and their corresponding temperature measurement locations which are equivalent to those used in the physical experiments. Note that in the images presented in Figure 10, the models have been cut in half in order to better visualize the through thickness temperatures.

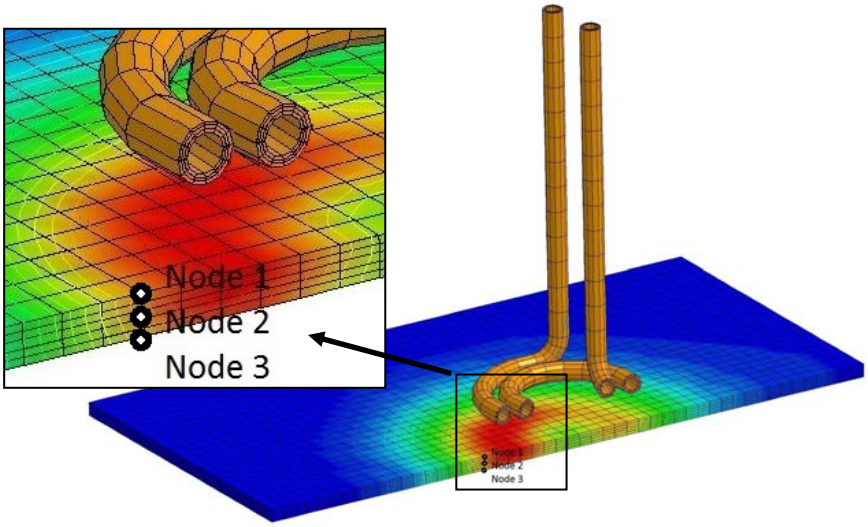

a)

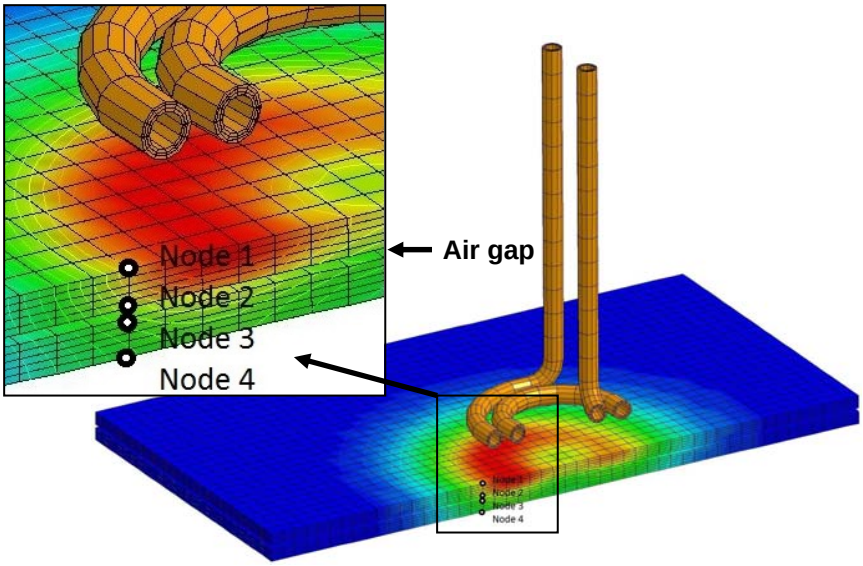

b)

Figure 10: *LS-DYNA R7 FEM/BEM simulation model set-up for a) single 2 mm and b) double 2 x 2 mm plate through the thickness temperature investigations and their corresponding point temperature measurement points*

In Figure 10 b) it can be seen that a small gap has been left between the plates in the double plate model. For this EM simulation case the interaction between three EM bodies is considered without the use of the EM contact card which is still currently in the beta development phase. In order for the EM solver to converge, the size of the gap must be no smaller than the thickness dimension of the solid finite elements used (i.e. the BEM element size adjacent to the gap). When the EM contact card is used, then no gap is required for convergence since the contact resistance is considered as part of the EM circuit. In this case, an extra Joule heating term according to Holm's equation [11] defining a contact resistance can also be implemented.

Point temperature heating results for the single plate model shown in Figure 10 a) are given in Figures 11 and 12. Note that the node locations (Node 1, Node 2, Node 3) shown in Figure 10 correspond to the location of thermocouples (T1, T2, T3 on the graph legend) used in the physical experiments presented in section 3. The heating of two plates is of more interest than one but adds further complications as it involves an extra load contributor (i.e. an extra plate) in the electromagnetic circuit. The eddy currents developed in the top plate are now also affected by the presence of the bottom plate as well as the coil. In the double plate simulation case, the temperatures at Nodes 2 and 3 are averaged in order to estimate the experimental temperature T2 at the joining interface.

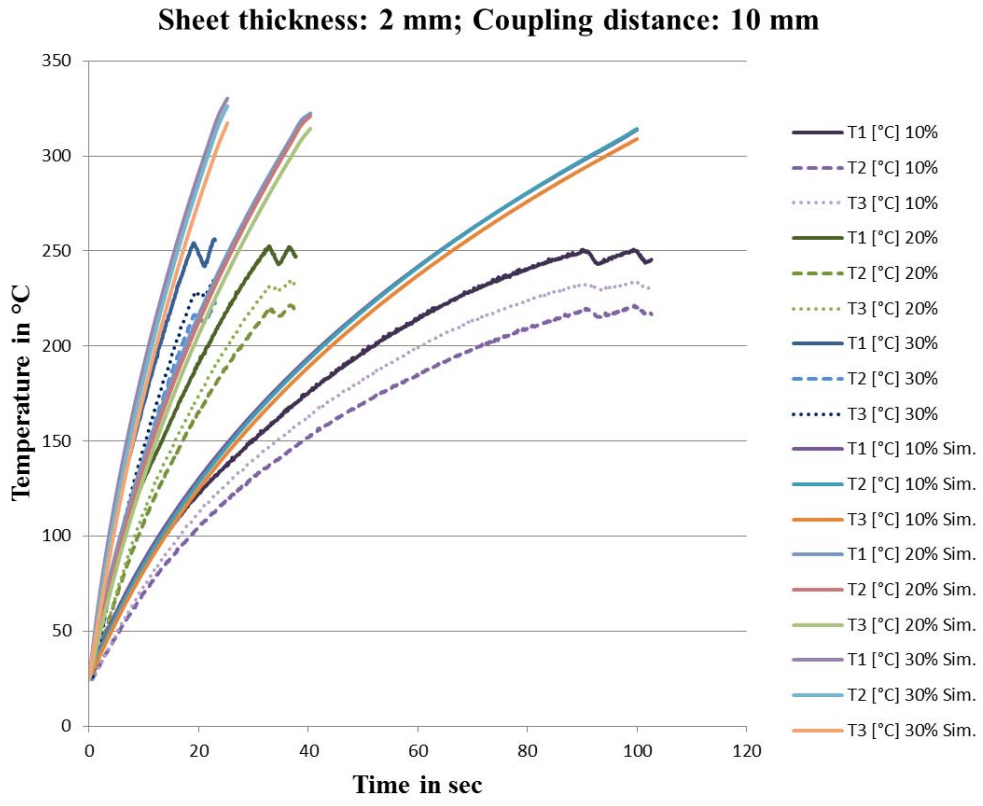

Figure 11: *Comparison between experiments and LS-DYNA simulation results for a 2 mm thick CF-PPS plate at 10 mm coupling distance for 10% (163 A), 20% (231 A) and 30% (283 A) power and coil frequency of 540kHz*

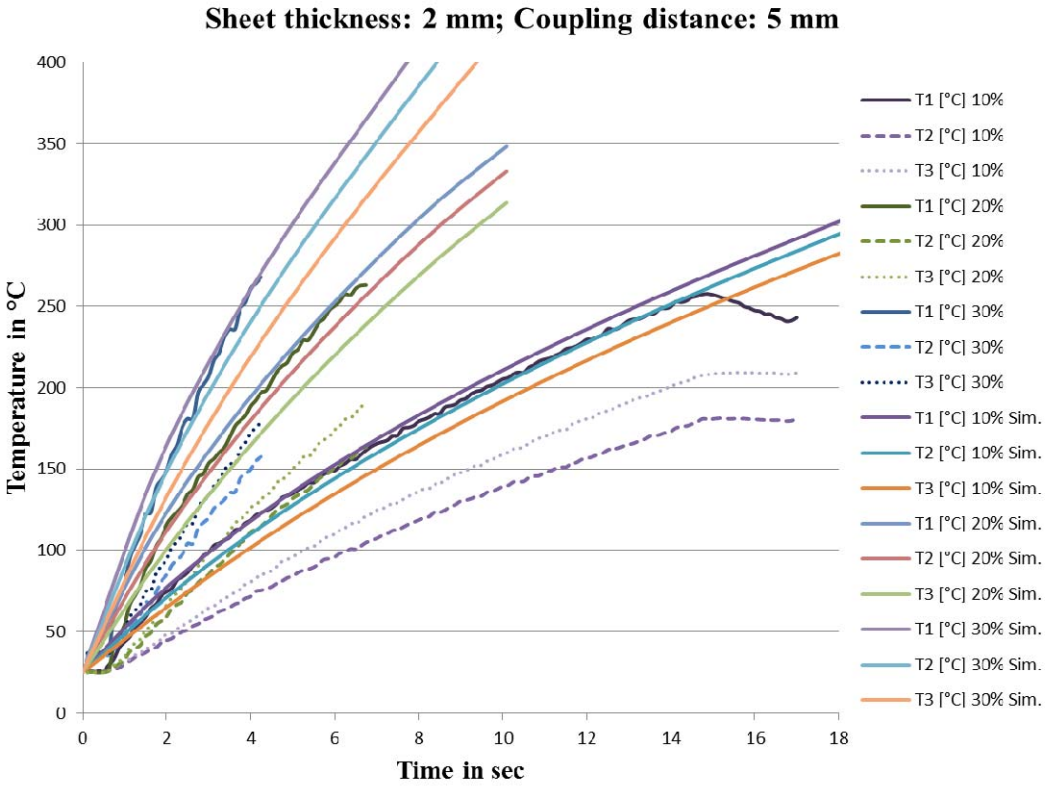

Figure 12: *Comparison between experiments and LS-DYNA simulation results for a 2 mm thick CF-PPS plate at 5 mm coupling distance for 10% (163 A), 20% (231 A) and 30% (283 A) power and coil frequency of 540kHz*

Based on the results from the simulations, the following comments can be made regarding the accuracy of the heating predictions for the single 2 mm plate (Figures 11 and 12). For the discussion it should be noted that in the current simulations a constant value of electrical conductivity was used.

For a coupling distance of 10 mm, it can be seen that the predictions are good at the beginning but tend to get worse over a larger temperature range and longer heating times. The reason for this could be the fact that the code uses a sinusoidal approximation for the shape of the oscillating current wave form when in fact the actual waveform deviates significantly from this shape. A solution to this is already planned via the implementation of an "actual" two-period current waveform, implemented as a curve based input replacing the current and frequency parameters in the EM_Circuit card. The actual two-period current versus time waveform (the same as required for the full eddy current solver) occurring on the coil can be measured using special electronic equipment and an oscilloscope and can then be output as a data file for use in the simulations. Another deviation in the prediction is the spread in the temperature curves T1-T3. This is briefly discussed in section 5.2 in terms of the implementation of a non-linear temperature dependent electrical conductivity which is also possible in the code via an equation of state (EOS) in the EM_MAT card. The EOS id in the EM_MAT card then links to a curve defining the electrical conductivity versus temperature.

For the closer coupling distance and shorter heating time results shown in Figure 12, the implementation of a non-liner electrical conductivity is believed to be more important as the through thickness temperature gradients are much larger. In Figure 12, it can be seen that the top surface (T1) temperature predictions are good but that the temperatures in the other two locations are over predicted.

In Figure 13, the results from the simulations of the 2 x 2 mm plate stack using the model shown in Figure 10 b) are compared with the experiments. Only the most relevant temperature location, T2, at the bonding interface has been compared for clarity. It can be seen that the prediction is again initially good but begins to deviate more and more at lower power levels and longer heating times.

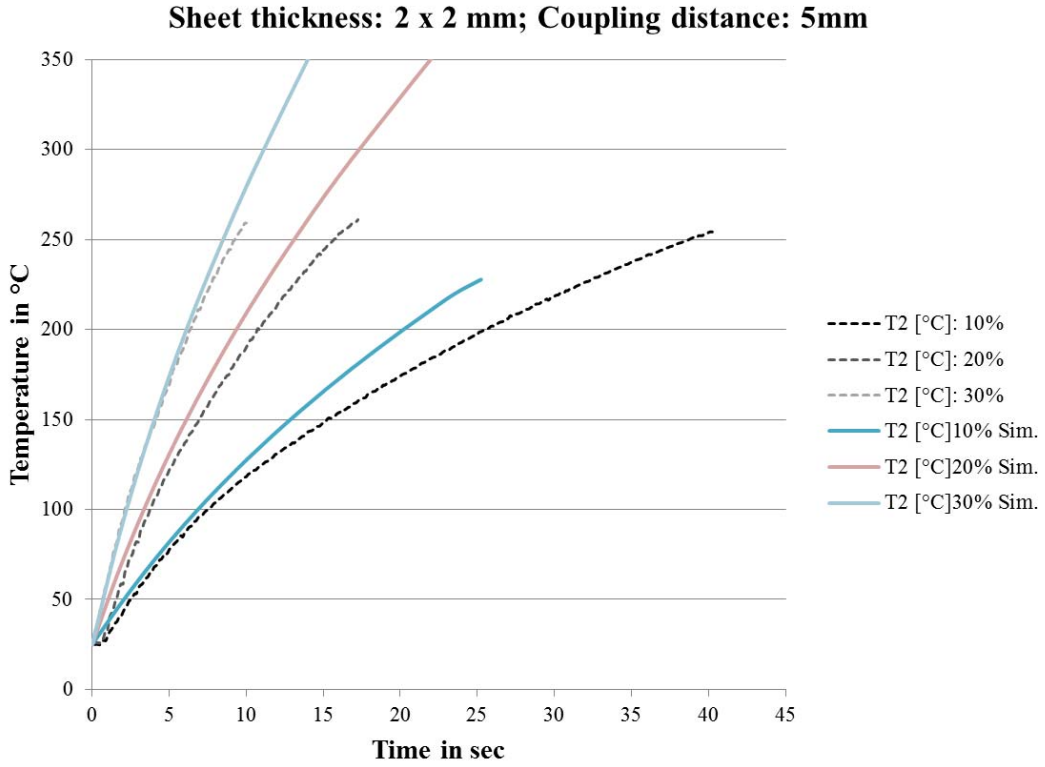

Figure 13: *Comparison between experiments and LS-DYNA simulation results for a 2 x 2 mm thick CF-PPS plate at 5 mm coupling distance for T2 only at 10% (163 A), 20% (231 A) and 30% (283 A) power and coil frequency of 540kHz*

The full set of simulation results for the 2 x 2 mm plate is given in Figure 14. A direct comparison can be made with the experimental curves obtained for the same parameter set shown earlier in Figure 7. Here it can be seen that the temperature at locations T1 and T3 are highly overestimated if the experimental results are assumed to be 100% correct. Further simulation versus experimental comparisons of a single 4 mm thick CF-PPS plate at 5 and 10 mm coupling distances were also performed. In this case, Figures 15 and 16 show very good overall predictions of the temperatures but again no sign of any non-linear type temperature rise in T1 or switching of the highest temperature location as was observed in the experiments.

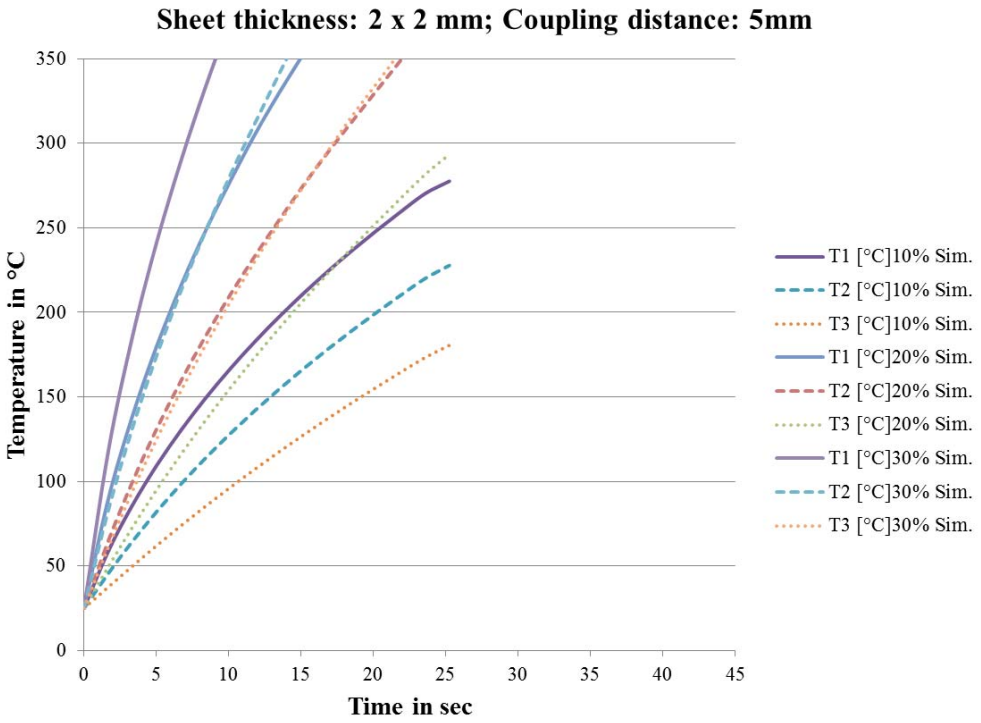

Figure 14: *LS-DYNA simulation results for a 2 x 2 mm thick CF-PPS plate at 5 mm coupling distance for all thermocouple locations T1- T3 at 10% (163 A), 20% (231 A) and 30% (283 A) power and coil frequency of 540kHz*

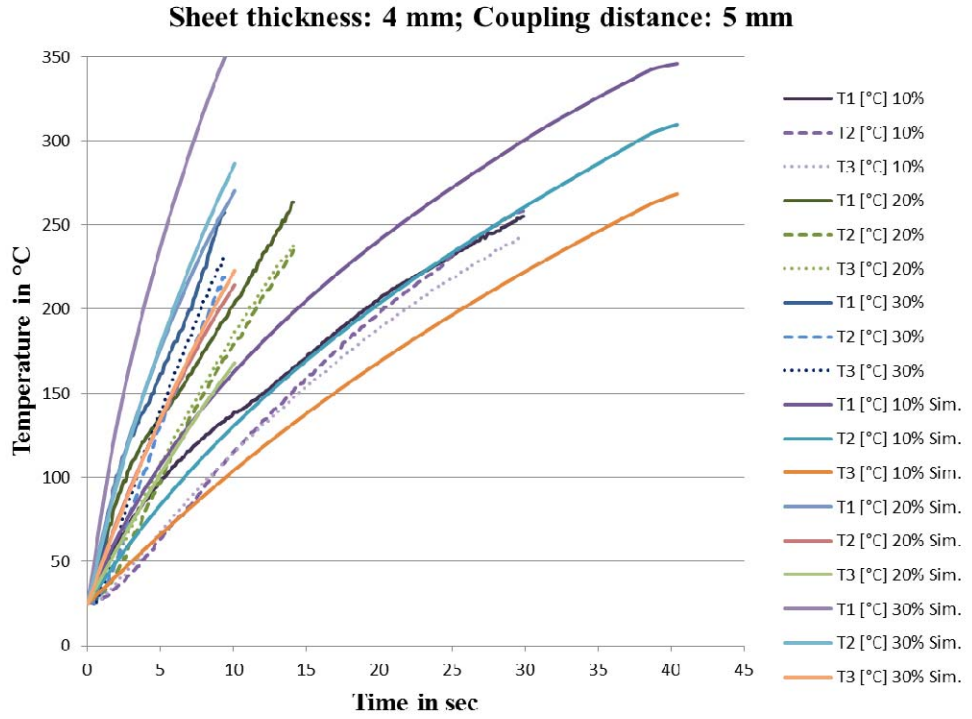

Figure 15: *Comparison between experiments and LS-DYNA simulation results for a single 4 mm thick CF-PPS plate at 5 mm coupling distance for 10% (163 A), 20% (231 A) and 30% (283 A) power and coil frequency of 540kHz*

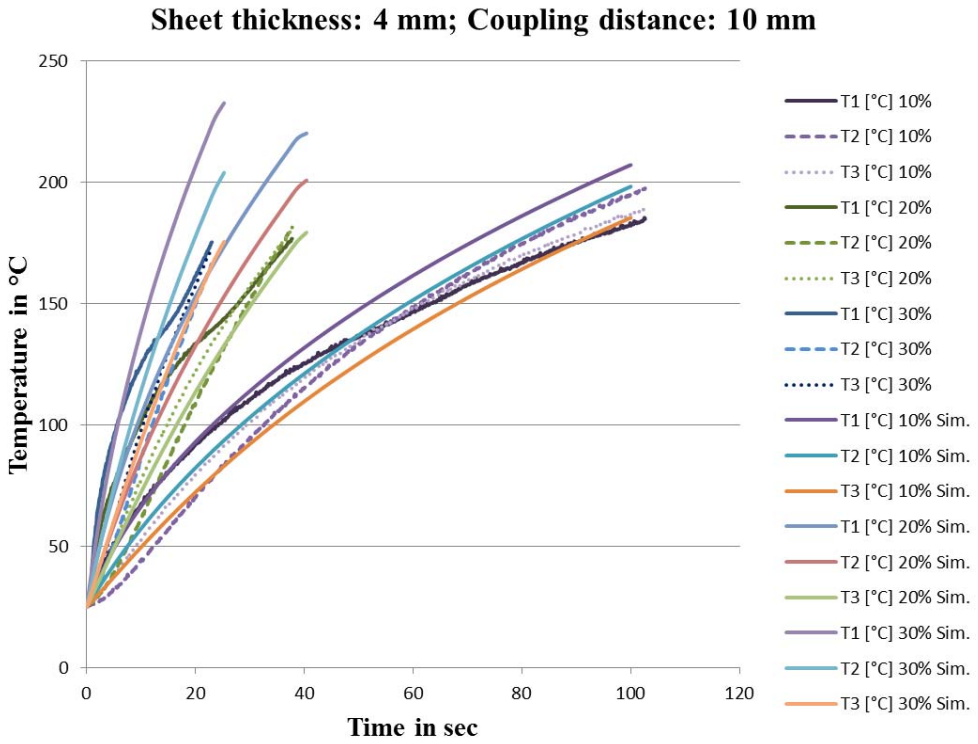

Figure 16: *Comparison between experiments and LS-DYNA simulation results for a single 4 mm thick CF-PPS plate at 10 mm coupling distance for 10% (163 A), 20% (231 A) and 30% (283 A) power and coil frequency of 540kHz*

It is very interesting to observe that in the simulations of 2 x 2 mm plates using the "gap" approach and no consideration of any contact resistance between the laminate stack, that the heating of the 2 x 2 mm material stack compared to a single 4 mm plate at the same coupling distance occurs faster. The difference however is small (21.9 sec versus 20.2 sec to 253°C for the 4 mm and 2 x 2 mm tests respectively) but is likely to be within the margin of error of the results. Preliminary implementation of the EM contact resistance card with Joule heating effect show much higher temperature predictions but still no "kinking" in the T1 temperature curves as observed experimentally for all tests but more prominently for the thicker material cases both connected and unconnected.

5-2 Influence non-linear electrical conductivity and orthotropic material input

In general, using a constant value of electrical conductivity over-predicts the heating effect over a wider temperature range as can be seen in Figures 11-16. By defining a non-linear electrical conductivity dependent on temperature, both the temperature spread through the thickness and the predictions over a large temperature range can be improved. This improvement however, comes at the expense of computing time as the electromagnetic fields must be recalculated enough times to capture the non-linearity.

Initial simulations performed to assess the significance of orthotropic electrical conductivity tend to suggest no difference in the heating behavior when the material is

considered electrically orthotropic as opposed to isotropic. In an isotropic case, the material is assumed to have an electrical conductivity equivalent in all directions to that measured in the in-plane directions. It can only be presumed that the large order of magnitude difference (~1000) between the in-plane and through the thickness electrical conductivity, combined with the large skin depth (more that the entire thickness of the laminate stack, see Eqn. 1) results in an insensitivity to the through thickness value of electrical conductivity. This means that a simpler (isotropic) electromagnetic material model can in this case be applied.

6-Conclusions

The following work has demonstrated further developments in the induction heating solver available in LS-DYNA R7. Focus was given here to the prediction of the through thickness temperature distribution in single and stacked CF-PPS thermoplastic composite plates of 1 and 2 mm thicknesses. At present the overall predicted Joule heating is good but several peculiarities which occur experimentally are not reproduced in the simulations. These are effects including the temperature on the plate surface closest to the coil becoming lower than the temperature measured in the middle or the non-coil side of the single laminate or laminate stack after a significant heating time at a temperature well below the melting temperature of the PPS polymer. It was suspected and discussed that material, temperature measurement and induction equipment effects may be responsible for the behavior. In order to help understand why the experiments deviate from the simulation in this respect, further experimental investigations using a very fine reinforcement structure will be performed together with two different types of induction heating equipment and temperature measurements with thermocouples and non-contact laser pyrometers. At present the simulations do not consider electrical and thermal contact between unconnected plates however this is currently being implemented to see what such effects then have on the through thickness heating behavior.

References

[1] D. Grewell, A. Benatar and J. Park. Plastics and Composites Welding Handbook. Hanser, München, 2003.

[2] V. Rudnev, D. Loveless, R. Cook and M. Black. Handbook of Induction Heating. Marcel Dekker, New York, USA, 2003.

[3] M. Duhovic, L. Moser, P. Mitschang, M. Maier, I. Caldichoury, P. L'Eplattenier. Simulating the Joining of Composite Materials by Electromagnetic Induction. In: Proceedings of the 12th International LS-DYNA Users Conference, Electromagnetic (2), Detroit, 2012.

[4] M. Duhovic, I. Caldichoury, P. L'Eplattenier, P. Mitschang, M. Maier. Advances in Simulating the Joining of Composite Materials by Electromagnetic Induction. In: Proceedings of the 9th European LS-DYNA Users Conference, Manchester, 2013.

[5] L. Moser. Experimental Analysis and Modeling of Susceptorless Induction Welding of High Performance Thermoplastic Polymer Composites, PhD thesis, Institute für Verbundwerkstoffe GmbH, Kaiserslautern, Germany, 2012.

[6] J. Schuster, D. Heider, K. Sharp, M. Glowania, Thermal conductivities of three-dimensionally woven fabric composites, Composites Science and Technology, Volume 68, Issue 9, July 2008, Pages 2085-2091.

[7] LS-DYNA Theory Manual, LSTC.

[8] *P. L'Eplattenier, G. Cook, C. Ashcraft, M. Burger, A. Shapiro, G. Daehn, M. Seith*, "Introduction of an Electromagnetism Module in LS-DYNA for Coupled Mechanical-Thermal-Electromagnetic Simulations", 9th International LS-DYNA Users conference", Dearborn, Michigan, June 2005.

[9] *P. L'Eplattenier, G. Cook, C. Ashcraft* , "Introduction of an Electromagnetism Module in LS-DYNA for Coupled Mechanical-Thermal-Electromagnetic Simulations", Internatinal Conference On High Speed Forming 08, March 11-12, 2008, Dortmund, Germany.

[10] M. Duhovic, I. Caldichoury, P. L'Eplattenier, P. Mitschang, M. Maier. Advanced 3D finite element simulation of thermoplastic carbon fiber composite induction welding. ECCM-16 - 16th European Conference on Composite Materials, Seville, Spain, June 22-26, 2014.

[11] R. Holm, Electrical Contacts-Theory and Applications, 4th ed., Springer Verlag, New York, 1967.